

An Interactive Many Objective Evolutionary Algorithm with Cascade Clustering and Reference Point Incremental Learning

Hongwei Ge, Mingde Zhao, *Student Member, IEEE*, Liang Sun, Zhen Wang, Guozhen Tan, Qiang Zhang, C.L. Philip Chen, *Fellow, IEEE*

Abstract—Researches have shown difficulties in obtaining proximity while maintaining diversity for solving many-objective optimization problems (MaOPs). The complexities of the true Pareto Front (PF) also pose serious challenges for the pervasive algorithms for their insufficient ability to adapt to the characteristics of the true PF with no priori. This paper proposes a cascade Clustering and reference point incremental Learning based Interactive Algorithm (CLIA) for many-objective optimization. In the cascade clustering process, using reference lines provided by the learning process, individuals are clustered and intraclassly sorted in a bi-level cascade style for better proximity and diversity. In the reference point incremental learning process, using the feedbacks from the clustering process, the proper generation of reference points is gradually obtained by incremental learning and the reference lines are accordingly repositioned. The advantages of the proposed interactive algorithm CLIA lie not only in the proximity obtainment and diversity maintenance but also in the versatility for the diverse PFs which uses only the interactions between the two processes without incurring extra evaluations. The experimental studies on the CEC'2018 MaOP benchmark functions have shown that the proposed algorithm CLIA has satisfactory covering of the true PFs, and is competitive, stable and efficient compared with the state-of-the-art algorithms.

Index Terms—Many-objective optimization, interactive evolutionary algorithm, incremental machine learning, clustering, decomposition.

I. INTRODUCTION

MANY real-world problems involve conflicting objectives to be optimized simultaneously [1]–[3]. With the population based features, multi-objective evolutionary algorithms (MOEAs) have shown promising performance in tackling multi-objective optimization problems with two or three objectives in a reasonable runtime by simultaneously approximating various parts of the true Pareto Front (PF) within one run [4].

Aiming to find a representative subset of the Pareto optimal solutions Set (PS), MOEAs pursue two basic goals - obtaining proximity and maintaining diversity,

where proximity ensures that the subset is close to the true PF in the objective space and diversity ensures that the finite individuals in the subset can well represent the distribution of the true PF in the entire extent. The way to carry out the two tasks has a crucial impact on MOEAs' optimization performance [5]. The traditional Pareto dominance-based algorithms for multi-objective optimization problems, such as NSGA-II [6], SPEA2 [7] and PESA-II [8], work well with two or three objectives. However, their performance noticeably deteriorates when four or more objectives are involved [9], [10], as the traditional Pareto dominance based strategies lose their effectiveness in many-objective problems (MaOPs). This deterioration in performance greatly motivates researchers to develop new methods and techniques to tackle the MaOPs [11]–[14], especially for real-world applications with many-objectives to be optimized that appear widely in the domains of industrial and engineering design [15]–[18].

When dealing with MaOPs, experimental and analytical results have demonstrated that there are some remaining drawbacks in the current MOEAs [9], [19]. It is hard for most traditional algorithms to perform well on both proximity and diversity. Some algorithms achieve high performance on diversity but low performance on proximity or vice versa. This phenomenon is widely addressed as the “conflict between the proximity and diversity”. Though proximity and diversity are not actually conflicting, the problem is aggravated in the existing algorithms with the increase of the number of objectives. The theoretical research of Teytaud has also shown that when dealing with MaOPs, the difficulties making the MOEAs diverge away from the PF [9], can cause their performance of the traditional Pareto dominance based MOEAs designed for few objectives to degrade to no better than random search for problems with 10 or more objectives involved [20], as the traditional Pareto dominance based strategies lose their effectiveness in high-dimensional objective spaces although it works well in low-dimensional objective spaces. This phenomenon is widely regarded as “dominance resistance”. As the proportion of non-dominated solutions increases substantially with the number of objectives, the traditional Pareto dominance fails to distinguish the desired indi-

H. Ge, M. Zhao, L. Sun, G. Tan and Q. Zhang are with the College of Computer Science and Technology, Dalian University of Technology, Dalian 116023, China (email: hwge@dlut.edu.cn).

Z. Wang is with the School of Mathematical Sciences, Dalian University of Technology, Dalian 116023, China.

C. L. P. Chen is with the Department of Computer and Information Science, University of Macau, Macau 999078, China.

viduals. Thus, insufficient evolution selection pressure is provided on the individuals, causing deterioration on the performance of proximity. Also, in higher-dimensional objective spaces, it is more difficult for the strategies used in traditional MOEAs to maintain the diversity of the population during the evolution process.

In this paper, we propose a cascade Clustering and reference point incremental Learning based Interactive Algorithm (CLIA) to address these problems of proximity and diversity appeared in the MaOPs.

The rest of this paper is organized as follows: Section II gives the background of researches on the MaOPs including the related works, the remaining drawbacks of them, and also explains the motivations of this paper. Section III gives the details of the proposed algorithm with focus on two interacting crucial processes. Section IV presents the experimental studies of the proposed algorithm CLIA, which include investigating the characteristics and comparing the results with other state-of-the-art algorithms on standard benchmark functions. Section V concludes the paper.

II. BACKGROUND AND MOTIVATIONS

A. Related Works and Remaining Drawbacks

Confronted by the new difficulties in MaOPs, the major approaches to address them can be summarized into the three following strategies: enhancing dominance, employing indicators and decomposition.

Generally, the algorithms that employ the strategy of enhancing dominance try to increase the evolution selection pressure which cannot be sufficiently supplied using only the traditional Pareto dominance based mechanisms in MaOPs by modification and/or combination with new ranking mechanisms. The attempts for modification, including relaxing or controlling the Pareto dominance relation such as ϵ -dominance [19], [21], [22], α -dominance [23], θ -dominance [24], ϵ -box dominance [25], dominance area control [26], k -optimality [27], *etc.*, have been conducted. However, the way to determine the proper relaxation degree remains as an open issue [28]. The efforts for developing new ranking criteria including average ranking [29], L -optimality [21], fuzzy-based Pareto dominance [30], [31], preference order rank [32]–[34], grid-based rank [35], distance-based rank [36], [37], rank-dominance [38], and density adjustment strategies [39], [40], clustering-ranking [41], *etc.*, have also been made to combine with the dominance relation. However, researches have shown that these different dominance based approaches focus evolution toward one or several subspaces and fail to produce solutions along the entire extent of the PF [40], [42].

The algorithms that employ the indicator strategy utilize indicators to evaluate the quality of the individuals instead of enhancing Pareto dominance. The ideas of indicator-based MOEAs were early introduced by Zitzler *et al.* [43] and Beume *et al.* [44], who used the performance indicators to guide evolutionary process. Break-

ing away from employing the dominance based strategies, the indicator-based algorithms convert the convergence and diversity of the individuals into designed performance indicators, such as the Hyper Volume (HV) [45]–[47], hyper area ratio [48] and R2-indicator [49], [50], the IGD-NS indicator [51] *etc.*. However, on one hand, researches have shown that the extensive computation for the indicators in MaOPs still remains as a bottleneck [52], though contributions such as [11], [53], [54] have been made to alleviate the computational burden. On the other hand, the performance of the indicators cannot be guaranteed, as it is hard to design indicators capable of representing the degrees of both proximity and diversity with many-objectives, as many indicators, just like the Pareto dominance, may lose their effectiveness as the number of objectives increases.

The algorithms that employ the decomposition strategy aim to simplify the original MaOPs by downsizing their objective spaces. Some decomposition-based algorithms use reference lines¹ as weight vectors to decompose the original MaOP into a bunch of scalar problems. The objective function of each sub-problem is an aggregation of all the objective functions that assigns a weight to each objective [56]. The most popular aggregation approaches include the Tchebycheff, the weighted sum and the boundary intersection methods [56] or newly proposed scalarizing functions [57], *etc.*. The diversity is maintained by specifying a set of well-distributed reference lines to guide the process of the evolution [11]. The representative algorithm in this category is MOEA/D [56], which converts multi-objective problems into several single objective scalar sub-problems and sub-problems are optimized collaboratively. Some researchers have tried to improve the MOEA/D by focusing on neighborhood structures [9], [19], self-adaptation mechanisms [19], *etc.*. Other decomposition based algorithms use reference lines or neighborhoods to segment the original objective space into a bunch of subspaces and deal with the subproblems separately and/or cooperatively in the subspaces. In the representative algorithm NSGA-III [55], the population diversity is maintained by reference lines and the proximity is controlled by Pareto dominance. In GrEA [35], grids are employed to decompose the original objective space into subspaces. Overall, despite the MOEAs based on decomposition achieve encouraging performance and fast runtime, limitations for most algorithms in this category are obvious in that the decomposition based strategies rely on the uniformity of reference lines to maintain the diversity during the evolution of the population. To assure such uniformity, decomposition based algorithms such as [55], [56], [58] often employ a predefined set of uniformly distributed reference points generated on a unit hyperplane in the objective space that represent the directions of the reference lines as the objective space

¹In this paper, “reference lines” have identical meanings to the ones in [55], referring to the quivers from the origin to the reference points generated for decomposition.

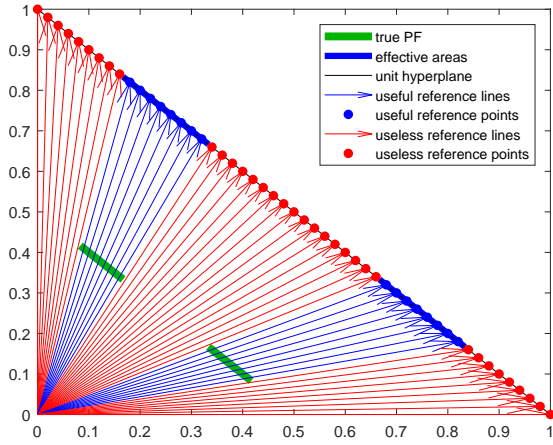


Fig. 1. Demonstration for the central projection of the true PF covering only parts of the unit hyperplane

is in a way decomposed into several evenly segmented subspaces. This method of reference point generation is proposed with the assumption that the reference lines that intersect with the unit hyperplane uniformly can also intersect with the true PF uniformly. In reality, this is hardly the case for the following two reasons. (1). The difference in curvature: The true PF may be irregular in shape, *e. g.* convex, concave or more complicated, so even if the reference lines intersect with the unit hyperplane uniformly, the intersection points with the true PF are not uniformly distributed for the difference in curvature [51], [58]. Since the shape of the true PF is not a known priori, researches have been conducted into the solutions of reference line adaptation [58]–[60]. However, as pointed out, though achieving significantly better performance on the problems with irregularly shaped PFs, their performance deteriorates when applied on the regular PFs, as the adaptation disturbs the uniformity of reference points [51]. (2). Partial PF: The central projection of the true PF from the origin to the unit hyperplane may cover only a part of the unit hyperplane regular hyper polygon (for convenience, the area is abbreviated as “the unit hyperplane”, this type of PF is recognized as “partial PFs”), as demonstrated in Fig. 1. The reference lines corresponding to the reference points generated outside the projection areas on the unit hyperplane hardly guide the evolution of non-dominated solutions near the true PF, since they do not intersect with the true PF. Thus, the number of useful reference lines is less than expected. This phenomenon can be observed vastly when the decomposition strategy is applied in the problems with discontinuous PFs where the uniformity is decreased due to the insufficiency of the intersection points of reference lines with the true PF. For this situation, reference points should be generated only inside the projection area on the unit hyperplane with density of expectation, so that the decomposition could be carried out properly.

Algorithms such as NSGA-III [55] and GrEA [35] employ more than one strategy above to enhance the

overall performance. Though still haunted by the inherent disadvantages of the strategies such as insufficient evolution selection pressure and sensitivity to reference lines etc., the comprehensive methods have brought competitive performance and versatility.

B. Motivations

Confronted by the mentioned difficulties, it is desirable to design an algorithm which embodies an efficient mechanism that could address problems in obtaining proximity and maintaining diversity with many-objectives, as well as a versatile mechanism that could handle various characteristics of diverse PFs.

In this paper, we propose a comprehensive algorithm CLIA that employs the strategy of enhancing dominance as well as the strategy of decomposition, with two interactive processes, the cascade clustering process and reference point incremental learning process, aiming to address the aforementioned problems with enhancements on both strategies.

In cascade clustering, using reference lines, solutions in the population are clustered and selected to obtain proximity and maintain diversity. The process is separately performed on the elite non-dominated solutions and other solutions in a cascade style, in which the cluster centers of elite non-dominated solutions guide the clustering of dominated solutions. Then intraclass ranking schemes are parallelly executed in each cluster. Picking only the elite non-dominated solutions as well as adopting the intraclass ranking could address the time-consumption. Finally, the round-robin picking maintain the proximity and diversity of the population. In general, if the reference lines are appropriately distributed, the proposed clustering process can effectively obtain proximity and maintain diversity within fair runtime.

The quality of reference lines, as we discussed above, has key impact on the performance of decomposition based algorithms. Employing an incremental learning classifier, the projection areas of the true PF on the unit hyperplane (the effective areas of reference point generation) are gradually estimated with the feedbacks from the clustering process. By increasing the density of reference point generation in the effective areas on the unit hyperplane, the reference points will be more properly generated, and the problem brought by the difference in curvature can be relieved since nearer intersection points over the true PF have smaller overall differences in curvature and the problem of partial PFs can be naturally solved. Addressing the sensitivity of the reference lines in the decomposition strategy, the proposed learning process ensures the performance of the cascade clustering.

Using reference lines that correspond to the more properly generated reference points from the reference point incremental learning process and providing feedbacks, the cascade clustering process interacts with the reference point incremental learning process as the algorithm proceeds.

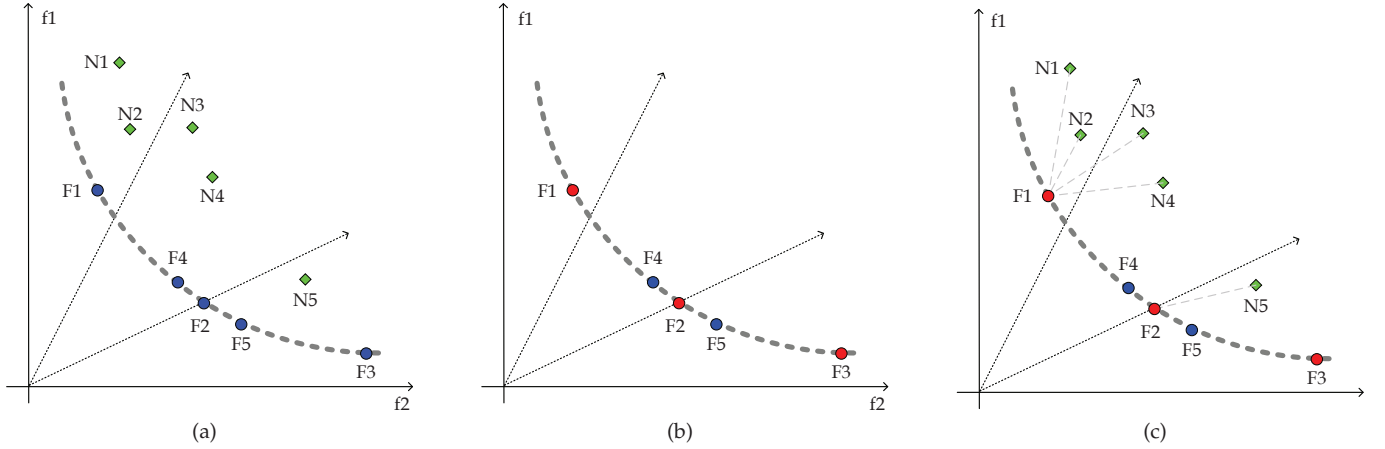


Fig. 2. Demonstration for the cascade clustering process: (a). Frontier solution identification. The identification segments the population into 2 parts: frontier solutions (F1 to F5) and non-frontier solutions (N1 to N5); (b). Cluster and sort the frontier solutions, locate the cluster centers (F1, F2 and F3). The frontier solutions attached to a mutual reference line are clustered and sorted using their PDM; (c). Cluster and sort the non-frontier solutions, create selection queues. The non-frontier solutions are attached to the existing clusters and sorted using their distances to the centers.

III. PROPOSED ALGORITHM CLIA

In this section, we will firstly introduce the basics of many-objective optimization problems and the key processes for multi or many-objective evolutionary algorithms. Then, the proposed algorithm CLIA will be explained with focus on the two crucial interactive processes. The first process is the selection operator based on cascade clustering, employed to guide the evolution of the individuals using the reference lines provided by the second process. The second is the reference point incremental learning process, employed to generate properly distributed reference lines using the feedbacks from the first process.

A. Basics

Given the objective function to be optimized is $\mathbf{f}(\mathbf{x}) = [f_1(\mathbf{x}), f_2(\mathbf{x}), \dots, f_M(\mathbf{x})]^T$, where M is the number of objectives. \mathbf{x} is a solution individual and $[f_1(\mathbf{x}), f_2(\mathbf{x}), \dots, f_M(\mathbf{x})]^T$ is the objective value of solution \mathbf{x} . Suppose $\mathbf{x}_1, \mathbf{x}_2$ are two solutions for the given problem, \mathbf{x}_1 **dominates** \mathbf{x}_2 iff $\forall i \in \{1, \dots, M\}, f_i(\mathbf{x}_1) \leq f_i(\mathbf{x}_2)$ and $\exists j \in \{1, \dots, M\}, f_j(\mathbf{x}_1) < f_j(\mathbf{x}_2)$. A solution \mathbf{x}^* is **Pareto optimal** if no solution in the feasible solution space S dominates it. Due to the conflicting nature of this kind of problems, often there is not only one optimal solution. The collection of all Pareto optimal solutions is called the Pareto Set (PS). The objective values of solutions in the PS constitute the true Pareto Front (PF), which is the limit of the evolutions of all solutions, as the objective value of no feasible point from the solution space dominates the points on the true PF.

The goal of MOEAs is to find a finite solution set X^* such that using the limited number of individuals, the objective values of them could be both a proximate and a diverse representative of the true PF.

The key processes of MOEAs include population initialization, population evolution and population selection. After the population is initialized as N uniformly distributed random points in the solution space, an evolution operator is applied on the population, creating an offspring population with the size of N . Together they constitute a potential population with a size of $2N$. Then the potential population is handed to the selection process to pick out the population of the next generation with the size of N . The evolution and selection processes cycle until the termination criteria are met.

B. Cascade Clustering

1) *Frontier Solution Selection*: Instead of using the traditional costly non-dominated sorting based on Pareto dominance relation for objective values of all solutions in every front, a *frontier solution identification* mechanism is employed, which only picks out the non-dominated solutions in the first front. For convenience, these solutions are called the *frontier solutions*, for they are the elite and the desirable solutions in the population.

2) *Bi-level Clustering and Intra-class Sorting*: Each frontier solution is attached to its nearest reference line by calculating DM , the sine values of the included angle of the objective value of the solution and all reference lines. Reference lines with frontier solutions attached are recognized as *active reference lines*. The frontier solutions belonging to the same active reference line are intra-classly sorted using the proposed proximity and diversity metric (PDM) in ascending order.

$$PDM(\mathbf{o}, \mathbf{r}) = PM(\mathbf{o}) + DM(\mathbf{o}, \mathbf{r}) = \text{mean}(\mathbf{o}) + \sin(\mathbf{o}, \mathbf{r}) \quad (1)$$

$DM(\mathbf{o}, \mathbf{r}) = \sin(\mathbf{o}, \mathbf{r})$ is the calculated sine value of the angle between the objective value of the frontier solution \mathbf{o} and the assigned active reference line \mathbf{r} (the vector from the origin to the reference point representing the direction for the reference line), representing the

Algorithm 1: Cascade Clustering

Input: R (reference points representing the reference lines), P_{old} (potential population), N (population size for the next generation)
Output: P (population for the next generation)

//Frontier Solution Identification
 $[F, NF] \leftarrow \text{FS_Identification}(P_{old});$
//Bi-level Clustering and Intra-class Sorting
for each frontier solution $f_i \in F$ **do**
 attach to reference line with smallest $\sin(r_j, f_i);$
 $PDM(f_i) \leftarrow \text{mean}(f_i) + \sin(r_j, f_i);$

for each active reference line $ar_i \in AR$ **do**
 Create a cluster c_i with all attached frontier solutions;
 $c_i.F \leftarrow \text{sort}(c_i.F, PDM(c_i.F), \text{ascend});$
 Pick out $c_i.f_j$ with the smallest PDM as $c_i.\text{center};$

for each non-frontier solution $nf_i \in NF$ **do**
 attach to cluster with the nearest center;

for each cluster $c_i \in C$ **do**
 $c_i.NF \leftarrow \text{sort}(c_i.NF, d(c_i.NF, c_i.\text{center}), \text{ascend});$
 Create selection queue $c_i.S \leftarrow \langle c_i.F, c_i.NF \rangle;$

//Round-robin Picking
 $i \leftarrow 1;$
 $C \leftarrow \text{shuffle}(C);$
 $P \leftarrow \emptyset;$
while $|P| < N$ **do**
 $P \leftarrow P \cup \text{Pop}(c_i.S);$
 $i \leftarrow \text{mod}(i, |C|) + 1;$

distribution error between the reference line r and the objective value of the frontier solution o . The smaller the overall DM , the closer the objective values of frontier solutions are to the reference lines. So, by using properly distributed reference lines, DM directs the evolution of individuals toward a better diversity. $PM(o)$ is a metric calculating the mean value of all components of the objective value vector, representing the proximity for the solution o . The smaller the overall $PM(o)$, the closer the frontier solutions are to the true PF. Similar to PBI in [56], PDM is also a metric and a decomposition approach to evaluate a preferred individual using the nearest reference line. The proximity term for PBI guides the evolution of individuals towards the origin, while PDM guides the evolution of individuals in a direction perpendicular to the unit hyperplane. The two directions both have the similar effect of pushing the objective values of solutions towards the true PF. However, the evolution direction of the proximity term of PDM is more even for the irregular PFs with long tails or sharp heads as the guiding directions are parallel towards the unit hyperplane. Also, the calculation of PDM is faster, that only mean values needs to be additionally calculated.

For each active reference line, the attached frontier solutions are gathered as a cluster. Also, the frontier

solution with the best PDM is taken as the center of the corresponding cluster. Each non-frontier solution is assigned to the clusters with the nearest cluster center. For each cluster, the non-frontier solutions are sorted by their Euclidean distances to the corresponding cluster centers in ascending orders. In this way, the objective values of the nearest frontier solutions are used to guide the evolution of the non-frontier solutions. By employing a criterion that does not select the solutions outside the first front as guiding solutions, a more intense pressure on evolution selection is obtained towards better proximity and better guidance for proximity is provided for the whole population. After these operations, clusters are created with two intra-classly sorted queues: the sorted frontier solution queue and the sorted non-frontier solution queue. The operations are graphically demonstrated in Fig. 2.

3) *Round-robin Selection:* For the proximity and the diversity brought by the desired frontier solutions and to enhance covering in the objective space by increasing the chance of selecting non-frontier solutions into the next generation, a round-robin picking method is employed. In each cluster, the selection queue is obtained by concatenating the sorted non-frontier solution queue after the sorted frontier solution queue. In each round, in a shuffled sequence, the head of each selection queue is popped out and added to the next generation until the size of the next generation reaches N . It should be noticed that, unless the clusters are more than N or replaced by better frontier solutions, *i. e.* new centers, all cluster centers are kept. This picking method ensures the inheritance of the desired frontier solutions as well as the diversity of picking the non-frontier solutions.

With M objectives and N individuals, frontier solutions are picked out in $O(MN^2)$, as $O(MN^2)$ is also costed on other operations including the bi-level clustering and intra-class sorting. Thus the overall runtime complexity for the process of cascade clustering is $O(MN^2)$, which is less costly compared to the non-dominated sorting based algorithms with $O(MN^3)$ costs [61].

The pseudo code of the cascade clustering process can be found in Algorithm 1.

Instead of being discarded, the attributes (active or not) of reference lines are gathered and handed to the reference point incremental learning process.

C. Reference Point Incremental Learning

Traditionally, reference points are evenly generated inside a hyper-polygon bounded with the points with unit intercepts on each objective over the unit hyperplane in the objective space with the expectation that the reference lines that go from the origin towards these points could intersect with the true PF uniformly. As discussed above, the central projection of the true PF (the effective areas for reference generation) from the origin to the hyperplane may cover just a part of reference points, *i. e.* the problem has a partial PF. When solutions

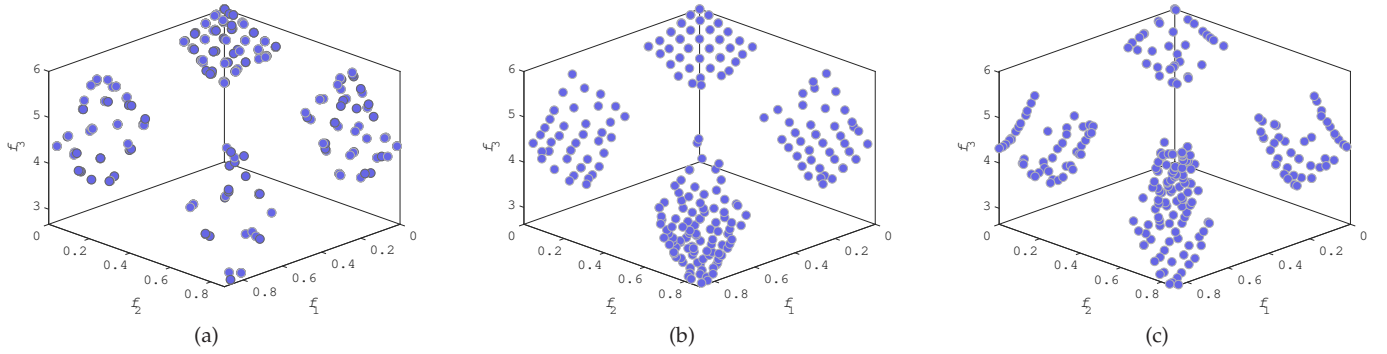


Fig. 3. Demonstration for the impact of the number of reference lines: (a). less reference lines than needed, some reference lines are overcrowded; (b). appropriate number of reference lines; (c). more reference lines than needed, only a part of reference lines are active.

evolve to be proximate to the true PF, the reference lines that intersect with the true PF are more likely to be the nearest to the solutions than the ones that do not intersect the true PF. When N reference points are uniformly generated on the unit hyperplane, the goal of cascade clustering is to select individuals out of N clusters with at least one solution assigned to one reference line. However, this cannot be done since less than N reference lines are actually properly distributed, *i. e.*, intersect with the true PF. Thus, a viable solution is to reduce the useless reference lines and increase the number of reference lines that intersect with the true PF, *i. e.*, to increase the reference points generated inside the effective areas on the unit hyperplane and reduce the outsiders that hardly make contributions.

An example is given in Fig. 1. When the reference points are evenly generated on the unit hyperplane, the reference lines are generated as lines that intersect with the origin and the reference points. However, as the example problem has a partial true PF, only a part of reference lines can intersect with the true PF, as shown in Fig. 1 where the reference lines intersecting with the true PF are in blue while others are in red. Thus, by a central projection from the origin, the true PF is projected on the unit hyperplane as the effective areas for the reference points. As it is shown in Fig. 1, the blue reference points are generated inside the central projection of the true PF from the origin on the unit hyperplane, while the red ones are not.

On one hand, if this is the case, that the density of reference lines is low and less than N reference lines go through the true PF, there will be less than N reference lines guiding the evolution of population. After selection, there will always be a reference line with more solutions than it is expected to attach. On the other hand, if the density of the reference points is too dense and the effective areas of the unit hyperplane are overcrowded with more reference points than needed, the solutions may unevenly attach to only a part of reference lines that go through only a part of true PF. To conclude, we should appropriately generate the reference points in the effective areas. The three situations are shown in Fig. 3.

In Fig. 3 (a), where insufficient reference points are generated in the effective areas of the unit hyperplane, it can be observed that though appropriately distributed, after selection, many reference lines are overcrowded with more than one solution. In Fig. 3 (b), where the reference points are appropriately distributed, it can be observed that the distribution of the solutions is relatively even in the true PF, which is the ideal case. In Fig. 3 (c), where too many reference points are generated, it can be observed that only a random part of reference lines are attached with solutions, causing a partial distribution of solutions near the true PF.

Generating more evenly distributed reference lines that could intersect with the true PF can both relieve the problems of brought by the differences in curvature of the true PF as well as the problems of insufficient useful reference lines brought by the partial PFs. Since the characteristics of the true PF is not a known *priori*, it can be imagined that it is hard to locate such effective areas on the unit hyperplane to generate reference points. However, since the individuals outnumber the active reference lines under such circumstance, the reference lines that intersect with the true PF are more likely to be attached with frontier solutions, *i. e.* the points corresponding to the active reference lines are more likely to be in the effective areas. This motivates us to use the attributes of the reference points to gradually estimate the distribution of the effective areas. However, since the shape of projection of the true PF on the unit hyperplane could be irregular, a definitive model for the boundaries should not be adopted for such complexities. Thus, the task should be finished with an implicit approach.

This task is carried out by a learning mechanism with a status sampler and a support vector machine. Whenever the distribution of active reference lines is stable, which means that in a period of cycles the active reference lines do not change, the sampler records and analyzes the attributes of all reference lines. If only a part of reference lines are active and the number of active reference lines is smaller than N , which means insufficient useful reference lines are generated, the reference points corresponding to the reference lines

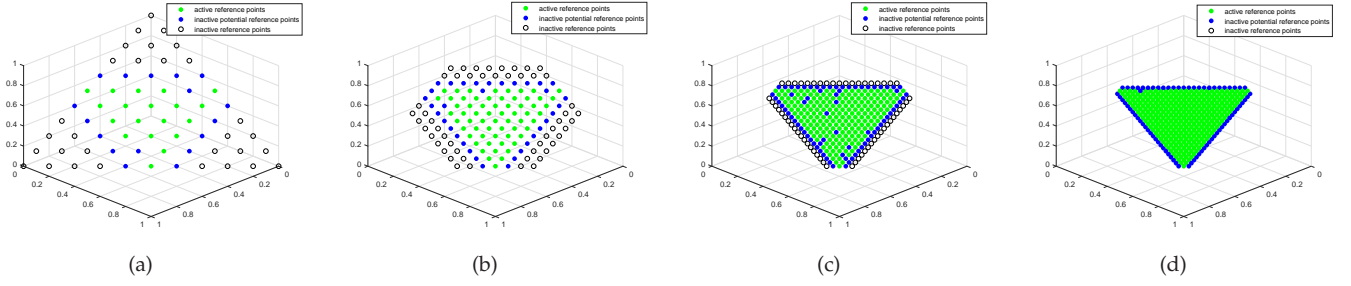


Fig. 4. Demonstration for the interactions of cascade clustering and reference point incremental learning: (a). Initial stage: N reference points are uniformly generated on the unit hyperplane; (b). Reference points are more densely generated and the low-scored ones are reduced using the scoring of the classifier whose knowledge is learnt from (a); (c). The process repeats: the number of active reference points gradually increases and the number of inactive reference points decreases; (d). The final status for reference point distribution: sufficient reference points are generated in the effective area.

will be marked with their attributes and be fed to a classifier for learning. Then the generation density for reference points is increased to generate more reference points and the old ones will be discarded. By employing Platt scaling [62], the output of the incremental learning classifier predicting whether a certain reference point is in the effective area or not can be converted into p , a score of probability distribution over classes. If $p > 0.5$, the reference point is considered as useful and vice versa. However, the learning may be inaccurate for many reasons. Thus, a threshold δ , $\delta < 0.5$, is employed to pick out the additional potential reference points whose $\delta \leq p < 0.5$. As it is discussed, the learning process may be initiated more than once. The old information of reference points is worthy of using, and the new attributes of reference points should also be learned. It is costly to archive all the old data and retrain the classifier for each learning process initiated, which is the exact case that incremental machine learning should be applied. So, we employ the incremental SVM for the situation.

The pseudo code for the redistribution process is in Algorithm 2.

Increasing the generation density of reference points in the effective areas ensures the versatility on the MaOPs with partial PFs and relieves the problems brought by the difference in curvature. It should be noticed as well that we do not have to use a definitive model for the boundaries of the projection of the true PF, an incremental learning classifier is used to gradually estimate the boundary of the effective area with no extra burden on the fitness evaluation of the population, as the information of learning comes from the feedbacks of the clustering process.

D. Demonstration for Clustering-Learning Interactions

Take a run of CLIA on the benchmark problem f_1 of the CEC'2018 MaOP competition [63] for the demonstration of the interactions of the two processes.

At first, N reference points are uniformly generated on the unit hyperplane using the traditional generation

Algorithm 2: Reference Point Incremental Learning

Input: ARP (active reference points), IRP (inactive reference points), S (sampler status), D (old reference point generation density), M (number of objectives), N (population size), δ (potential threshold), B (bases of hyper projection)

Output: new reference points RP , new generation density D

```

if isStable( $S$ ) and  $|ARP| < N$  then
  //Incremental learning after hyper projection
  Classifier = IncrementalLearn(Classifier,
    HP( $ARP$ ), HP( $IRP$ ));
  //Generate denser reference points
   $D = D + 1$ ;
   $RP = \text{generateReferencePoints}(D, M)$ ;
  //pick the points with  $p \geq \delta$ 
   $RP = \text{ClassifierPick}(\text{Classifier}, \text{HP}(RP), \delta)$ ;

```

method identical to [55] and their corresponding reference lines are handed to cascade clustering for population selection. Then, the selection operator additionally returns the attributes of the reference lines. The active reference points corresponding to the active reference lines (the reference lines with frontier solutions attached) are marked in green, while the other reference points are inactive, as it is shown in Fig. 4 (a). If the sampler considers this status stable, when the attributes of reference points are relatively reliable for learning, the attributes of all current reference points will be sent to the classifier for incremental learning. However, since the reference points are all located on the unit hyperplane, which is one dimension lower than the objective space, a hyper projection is firstly applied on the coordinates of the reference points to decrease their dimensionality. At the initialization phase of the algorithm, the projection bases for the hyper projection process are firstly calculated and saved for the later processes using the center and the vertices of the regular hyper polygon on the unit hyperplane by the orthogonalization process of Jorge

Gram and Erhard Schmidt [64]. After the learning is complete, using the Platt scaling scoring scheme [62], the incremental learning classifier is able to identify the potential of a reference point (actually the projection of the reference point using the aforementioned bases) by scoring it. In Fig. 4 (a)(b)(c)(d), the blue points are the potential inactive reference points located in the potentially effective area of the unit hyperplane with scores greater or equal to δ . Considering that there are not enough active reference lines, more reference points are generated using a higher generation density. By applying the classifier on the newly generated reference points, the points with lower score than threshold, the ones not likely to be active, are reduced. Only the points with scores higher than or equal to δ are kept for the next clustering process. In Fig. 4 (b), as it is demonstrated, the reference points located at the tails of the triangle area are reduced for their low scores, only the reference points with scores greater than or equal to δ are participating the clustering process. Whenever the sampler considers the status of reference lines stable and the number of current active reference points is below N , the above process repeats, as it is demonstrated in Fig. 4 (c)(d). As the process repeats, more accurate boundaries for classification can be obtained, since the population is getting nearer to the true PF and the intermediate areas on the unit hyperplane are filled with denser data points. If the clustering process reports that the number of active reference lines is almost or above N , the reference point incremental learning process including the sampler, the incremental learning classifier and the reference point generator is disabled.

E. Proposed Framework

The framework of the proposed algorithm is formulated as the flowchart in Fig. 5.

First, to initialize, N individual solutions are randomly generated in the solution space S and N reference points are uniformly generated on the unit hyperplane in the objective space O representing the direction for N reference lines. Then, the main loop cycles until the criteria of termination are satisfied: evolve to get the offsprings using the N solutions in the population and obtain the potential population with a size of $2N$. Then, out of the potential population, using the selection operator based on cascade clustering, the new population with the size of N is picked out. Then the information of feedbacks of the clustering process is additionally used. If the number of active reference lines are not enough, an incremental classifier will learn from the stable status and locate the potential areas for the newly denser generated reference points. The algorithm proceeds along with interactions of the cascade clustering process and the reference point incremental learning.

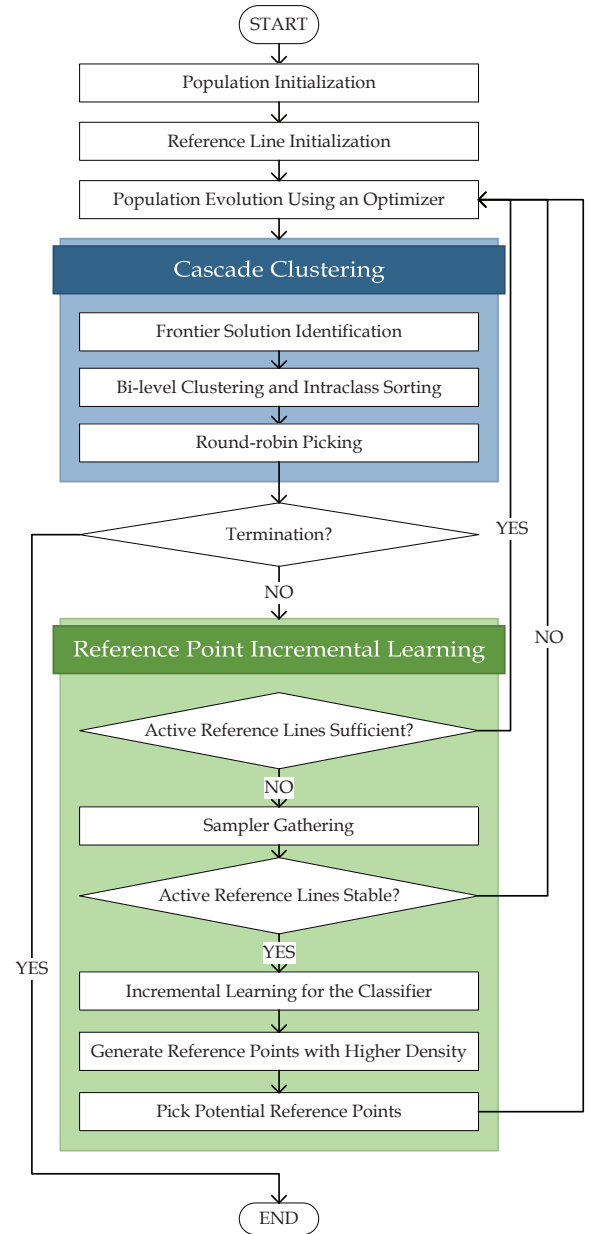


Fig. 5. The Framework of the Proposed Algorithm CLIA

IV. EXPERIMENTAL STUDIES

A. Experimental Settings

To demonstrate the effectiveness of CLIA, the benchmark suite for CEC'2018 MaOP competition is chosen, which is designed for understanding the strengths and weaknesses of MOEAs with benchmark functions of diverse characteristics [63]. In the technical report for CEC'2018 MaOP competition, 15 many-objective benchmark functions (MaF) are provided with box constraints in the solution space. For each of the 15 benchmark functions, there are three separate test cases, $M = 5$, $M = 10$ and $M = 15$, constituting 45 different test cases. With official standards including using the default simulated binary crossover and polynomial mutation optimizer with default parameters and the population

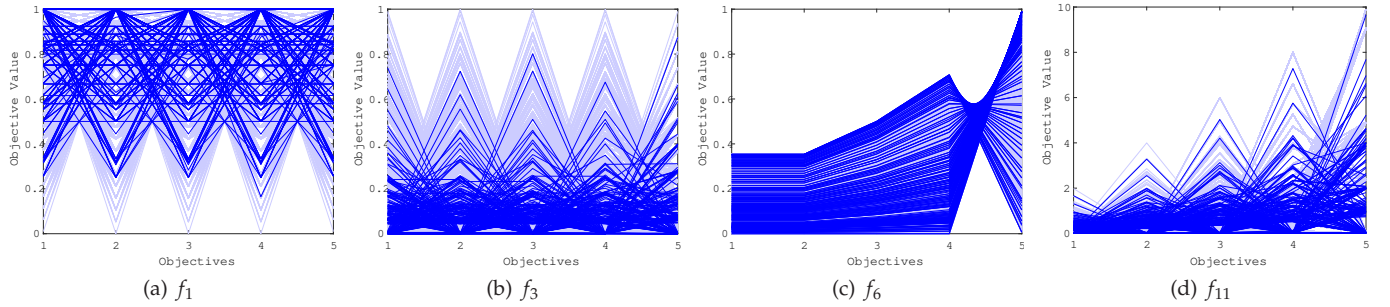


Fig. 6. Demonstration for the covering of the final population on the true PF on 5 benchmark functions

size of $N = 240$ and the designated number of fitness evaluations, all data of each algorithm given in this section is averaged over 20 independent runs for each test case on PlatEMO [65]. The settings of the experimental studies in this paper are identical to the standard for CEC'2018 MaOP competition, which can be found in [63], together with the details of the benchmark functions.

An incremental learning SVM with a Gaussian kernel, kernel scale of 0.56 and the soft-margin regularization parameter of $C = 10$ is adopted. The details of its parameter settings can be found in [66].

In our implementation, threshold δ is dynamically set to be the score of reference point with the $\min(R, 2N)$ -th highest score, *i. e.*, when the number of active reference lines is below N , after a denser generation of reference points with totally R in number, at least $\min(R, 2N)$ reference points will be kept. Thus, at least $\min(R, 2N)$ reference points are continuously redistributed to the potential areas unless the disabling criteria are met.

All data obtained is run on a computer with a quad core 3.5 GHz 8-Gen Core i7 CPU and 16.0GB of memory on MATLAB R2017b. The source code of CLIA is implemented using the open source PlatEMO [65] with compatibilities for MATLAB R2017b².

B. Performance Metrics

The two prevailing metrics to evaluate the quality of a solution population are IGD and HV.

Originally used in [67], IGD, short for Inverted Generational Distance, is a comprehensive measure of both proximity and diversity of a population. Let P^* be a set of evenly distributed sample points over the true PF and P be the current population, the n -order IGD from P to P^* can be formulated as:

$$IGD(P, P^*, n) = \frac{(\sum_{v \in P^*} d^n(v, P))^{1/n}}{|P^*|} \quad (2)$$

where $d(v, P)$ is the minimum Euclidean distance between a sample point v on the true PF and the solutions in P . Originally, when IGD is first used in evaluating the performance of MOEAs [68], [69], n is taken as 2, *i. e.*,

the 2-order IGD is adopted. In the recently papers, n is widely chosen as 1 as it is in [51]. In this paper, to concur with the metrics of the CEC'2018 MaOP competition [63], n is also taken as 1. When $|P^*|$ is large enough, $IGD(P, P^*, 1)$ can measure both the diversity and the proximity of P . The smaller the IGD, the better the proximity and diversity.

Calculating the volume of the objective space between the obtained solution population and a reference point, HV, short for HyperVolume, can give the set a comprehensive assessment in terms of proximity and diversity [70]. For clarity and the consistency with the CEC'2018 MaOP competition, the normalized HV (NHV) [63] is adopted to normalize the hypervolume to the interval $[0, 1]$. The higher the NHV, the better the size of the space covered, the better proximity and diversity.

C. Characteristic Studies

1) *Covering of the true PF*: In Fig. 6, the objective values of all individuals for 5 test cases are plotted in parallel coordinates, with the Y-axis representing the objective values on each objective and the X-axis representing the specified objectives. Also, in the bottom layer of the subfigures, the objective values of the sampled true PFs are plotted in a lighter color. These graphs in Fig. 6 provide an intuitive demonstration for the performance of an MOEA on the covering of the true PF. With the limited size of population, the ideal performance is to find the solutions whose objective values are evenly distributed over the true PF in each objective in the parallel coordinates. However, though showing satisfactory covering, it can be observed that the objective values of individuals found by CLIA is not ideal since they are distributed over the PF in a messy way and some objectives are outside the PF area showing unsatisfactory proximity.

It can be observed from Fig. 6 that some representative individuals with extreme objective values on certain objectives are missed by the proposed algorithm CLIA. This can be ascribed to the fuzzy boundaries of the effective areas on the unit hyperplane, since the results of the process of reference point incremental learning are not completely accurate. The inaccurate scoring on the boundaries of the potential effective areas may lead

²The MATLAB source code can be found in Mingde Zhao's github: <https://github.com/PwnerHarry/>

to the loss of some useful reference points, causing the aforementioned problems.

TABLE I
THE COMPARED ALGORITHMS AND THE CORRESPONDING STRATEGIES

	Dominance	Indicator	Decomposition
CLIA	Y		Y
AR-MOEA		Y	
NSGA-III	Y		Y
NSGA-II	Y		
IBEA		Y	
GrEA	Y		Y
KnEA	Y		
MOEA/D			Y
RVEA			Y

D. Comparative Studies

1) *Data on CEC'2018 MaOP Benchmark Suite*: The obtained data of IGD and NHV on each test case are compared with the corresponding data of the highlighted state-of-the-art algorithms in the PlatEMO platform including the AR-MOEA [51], NSGA-III [55], NSGA-II [6], IBEA [43], GrEA [35], KnEA [12], MOEA/D [56] and RVEA [58]. The characteristics of the compared algorithms are presented in Table I. The IGD and NHV results on CEC'2018 MaOP benchmark of CLIA and the 8 compared algorithms averaged over 20 independent runs are presented in Table II and Table III, respectively. For each test case, the result of with the best performance is barked in bold.

Friedman tests are also respectively conducted on the IGD results and the NHV results, the rankings and the detailed results are also presented in Table II and Table III. On IGD, $\chi^2 = 68.81$ and $p = 8.48 \times 10^{-12}$. On NHV, $\chi^2 = 54.92$ and $p = 4.58 \times 10^{-9}$. With the significance level of $\alpha = 0.05$, the Friedman test shows that the two respective rankings are effective since the differences of the results among the 9 algorithms are statistically significant. With the significant statistical differences, the proposed algorithm CLIA achieves the highest performance by obtaining the top overall ranking in both IGD and NHV considering all 45 individual test cases. The rankings with the best performance (lowest mean values of IGD, highest mean values of NHV) are marked in bold.

Two-sample *t*-tests are also conducted on the 8 pairs of algorithms, each pair is the proposed algorithm CLIA and one compared state-of-the-art algorithm. The results of the *t*-tests are provided as "*l/u/g*", where *l* represents the mean value of the proposed algorithm, for a certain test case, is significantly *less* than the compared algorithm, *g* represents a *greater* result, and *u* represents that it is *uncertain* to say whether the mean value of the proposed algorithm CLIA is greater or less than the compared algorithm. The *t*-test results where proposed algorithm CLIA performed better in number of test cases are marked in bold.

E. Categorized Performance Comparison and Analysis

With $M = 5$, the proposed algorithm CLIA outperforms other algorithms by ranking the 1st in 13 benchmark functions out of 15 with IGD and the 1st in 7 functions with NHV. Though still achieving competitive overall performance with $M = 10$ and $M = 15$, the deterioration for the performance of CLIA can be observed. The interval of performance rankings provided by Friedman test shrinks, showing that all compared algorithms still cannot fully address the problems with such number of objectives. For proposed algorithm CLIA, this may be resulted by the sparse distribution of the reference points in the high-dimensional objective space which is insufficient for the classifier to obtain the correct boundaries for the effective area over the unit hyperplane.

When dealing with the 8 functions with partial PFs whose projections do not fully cover the unit hyperplane ($f_1, f_2, f_4, f_6, f_7, f_8, f_9$ and f_{15}), CLIA obtains the best overall performance in both IGD and NHV with three different numbers of objectives, demonstrating that the process of reference point incremental learning has brought versatility for the diverse PFs.

On problems with PF projection fully covering the unit hyperplane ($f_3, f_{10}, f_{11}, f_{12}, f_{13}$ and f_{14}), CLIA obtains the best overall performance on IGD and the second best on NHV on test cases of $M = 5$, $M = 10$ and $M = 15$, demonstrating the effectiveness of the selection operator based on cascade clustering.

On the large-scale problems (f_{14} and f_{15}), where the dimensionality of the solution space is relatively high, CLIA also achieves the highest overall performance with respect to the two metrics considering all test cases comprehensively.

Fig. 7 presents two radar diagrams specifying the rankings of the performance on each type of functions of the compared algorithms with the metrics of IGD and NHV respectively. In the IGD radar diagram Fig. 7 (a), the values of the dimensions are the reciprocal rankings of obtained by the Friedman tests on each category of functions. In the NHV radar diagram Fig. 7 (b), the values of the dimensions are the rankings of obtained by the Friedman tests on each category of functions. For the category "M5", "M10" and "M15", the results of the test cases of all 15 benchmark functions of $M = 5$, $M = 10$ and $M = 15$ respectively are analyzed by the Friedman mean ranking process. For the functions of a certain category, the data of those functions under $M = 5$, $M = 10$ and $M = 15$ are all taken to Friedman tests. The rankings for "M5", "M10" and "M15" can be found in Table II and Table III.

F. Runtime Comparison and Analysis

Table IV provides the runtime of all the compared algorithms as well as ratios of their runtime to the runtime of the proposed CLIA. In the table, the "runtime" is all averaged over 20 independent runs as the total runtime needed for running all 15 benchmark functions

TABLE II

STATISTICS FOR IGD: MEAN, STD, FRIEDMAN MEAN RANKS AND *t*-TESTS OF 9 ALGORITHMS AVERAGED USING 20 INDEPENDENT RUNS

	CLIA		AR-MOEA		NSGA-III		NSGA-II		IBEA		GrEA		KnEA		MOEA/D		RVEA		
	Mean	Std	Mean	Std	Mean	Std	Mean	Std	Mean	Std	Mean	Std	Mean	Std	Mean	Std	Mean	Std	
<i>f</i> ₁	5	1.12e-1	2.54e-4	1.41e-1	1.89e-3	1.97e-1	1.42e-2	1.73e-1	2.15e-3	1.45e-1	5.44e-3	1.35e-1	1.35e-3	1.24e-1	2.44e-3	2.34e-1	1.84e-2	3.07e-1	3.81e-2
	10	3.10e-1	2.11e-3	2.52e-1	1.29e-3	2.67e-1	5.64e-3	2.92e0	1.03e-2	2.74e-1	5.82e-3	2.49e-1	8.79e-3	2.31e-1	1.56e-3	4.68e-1	4.35e-4	6.76e-1	7.00e-2
	15	3.19e-1	3.43e-3	2.88e-1	1.25e-2	3.17e-1	2.24e-3	3.37e-1	1.01e-2	3.16e-1	1.89e-3	3.38e-1	1.96e-2	2.76e-1	3.27e-3	5.77e-1	3.83e-3	6.89e-1	8.79e-2
<i>f</i> ₂	5	9.60e-2	1.55e-3	1.11e-1	1.03e-3	1.29e-1	2.31e-3	1.43e-1	3.02e-3	1.09e-1	1.22e-3	1.13e-1	1.54e-3	1.29e-1	3.65e-3	1.24e-1	5.38e-4	1.29e-1	2.42e-3
	10	1.95e-1	1.10e-2	2.06e-1	8.73e-3	2.41e-1	4.40e-2	1.63e-1	2.31e-3	1.90e-1	1.33e-2	4.02e-1	1.31e-2	1.56e-1	2.21e-3	3.24e-1	1.78e-3	2.36e-1	9.08e-3
	15	2.98e-1	1.32e-2	2.26e-1	1.02e-2	2.08e-1	7.50e-3	1.75e-1	3.91e-3	2.96e-1	7.83e-3	3.69e-1	6.38e-3	1.79e-1	8.30e-3	3.63e-1	3.47e-4	6.84e-1	2.38e-1
<i>f</i> ₃	5	7.11e-2	8.28e-3	9.71e-2	1.74e-3	1.08e-1	2.38e-2	2.86e-1	7.70e-3	5.83e-1	3.29e-1	7.13e-1	2.62e-1	1.53e-1	4.01e-2	1.25e-1	2.27e-3	8.37e-2	7.15e-3
	10	8.28e-2	7.23e-3	4.08e0	1.18e+1	2.66e+2	1.21e+2	2.37e+6	1.31e+6	3.46e-1	6.27e-2	4.59e+2	6.07e+2	1.67e+8	3.44e+8	1.45e-1	1.14e-3	8.51e-2	2.87e-3
	15	8.91e-2	9.77e-4	5.48e+1	1.51e+2	1.88e-1	7.14e-2	2.47e+6	1.07e+6	2.65e-1	6.06e-2	6.52e+2	6.04e+2	1.28e+9	1.55e+9	1.31e-1	3.15e-4	1.21e-1	2.50e-2
<i>f</i> ₄	5	2.02e0	1.04e-1	2.45e0	9.25e-2	3.21e0	3.43e-1	2.23e0	9.26e-2	5.81e0	6.66e-1	2.20e0	1.12e-1	3.07e0	3.86e-1	9.66e0	3.08e-1	4.88e0	9.44e-1
	10	8.50e+1	6.46e0	9.68e+1	6.42e0	9.73e+1	9.12e0	5.94e+1	4.35e0	1.65e+2	1.02e+1	1.61e+2	1.64e+1	7.59e+1	8.38e0	4.45e+2	1.55e+1	2.34e+2	2.69e+1
	15	3.71e+3	1.82e+2	4.01e+3	5.26e+2	4.17e+3	2.07e+2	1.62e+3	1.13e+2	4.51e+3	1.81e+2	5.00e+3	1.75e+3	1.80e+3	3.18e+2	1.90e+4	6.18e+2	7.23e+3	1.00e+3
<i>f</i> ₅	5	2.10e0	3.92e-1	2.39e0	8.01e-1	2.21e0	1.75e-3	2.29e0	3.21e-2	2.34e0	3.20e-2	1.28e-1	2.48e0	9.56e-2	2.73e0	9.59e-2	1.58e-1	8.15e-2	2.45e-2
	10	8.67e+1	1.33e+1	9.87e+1	4.11e0	8.81e+1	6.82e-1	9.53e+1	4.15e0	5.88e+1	2.75e0	4.82e+1	1.45e0	7.63e+1	1.15e+1	3.01e+2	1.72e0	1.03e+2	6.63e0
	15	2.34e+3	4.85e+2	3.31e+3	4.44e+2	2.59e+3	1.73e+2	1.72e+3	6.39e+1	1.32e+3	4.97e+1	1.09e+3	5.02e+1	1.71e+3	1.31e+2	7.32e+3	4.42e-1	2.94e+3	2.04e+2
<i>f</i> ₆	5	5.76e-3	2.72e-4	4.22e-3	5.63e-5	4.40e-2	1.49e-2	4.66e-3	2.70e-4	6.07e-2	2.04e-2	3.75e-2	1.33e-3	8.09e-3	3.73e-3	9.59e-2	1.58e-1	8.15e-2	2.45e-2
	10	4.62e-2	2.30e-3	1.08e-1	1.40e-1	2.16e-1	8.80e-2	3.85e-1	3.28e-2	1.65e-1	1.62e-1	3.93e-1	8.53e-2	9.78e0	4.60e0	1.23e-1	2.06e-1	1.37e-1	1.67e-2
	15	6.28e-2	6.70e-2	2.38e-1	1.25e-1	3.17e-1	4.27e-2	6.20e-1	6.65e-1	3.92e-1	7.97e-2	1.29e0	8.32e-1	2.53e+1	2.63e+1	1.85e-1	1.03e-1	1.20e-1	2.37e-2
<i>f</i> ₇	5	2.87e-1	3.32e-2	3.29e-1	7.55e-3	3.28e-1	1.12e-2	3.59e-1	3.69e-3	3.07e-1	1.41e-2	2.65e-1	3.00e-3	2.90e-1	1.45e-2	1.08e0	2.27e-2	4.49e-1	1.01e-3
	10	9.79e-1	9.83e-2	1.57e0	9.55e-2	1.02e0	6.51e-2	1.82e0	1.57e-1	9.04e-1	1.10e-1	2.49e0	1.15e-1	8.67e-1	1.45e-2	2.00e0	2.51e-1	2.96e0	3.53e-1
	15	2.72e0	3.40e-1	4.06e0	6.97e-1	4.74e0	1.13e0	3.26e0	3.46e-1	2.47e0	5.92e-1	6.82e0	9.20e-2	2.54e0	3.56e-1	4.09e0	6.85e-1	3.95e0	9.74e-1
<i>f</i> ₈	5	8.82e-2	3.12e-3	1.29e-1	1.45e-3	2.35e-1	1.81e-2	1.52e-1	7.69e-3	9.20e-1	6.36e-2	1.51e-1	6.35e-3	2.59e-1	1.04e-1	2.95e-1	9.11e-3	4.56e-1	2.47e-2
	10	4.49e-1	1.24e-1	1.37e-1	4.17e-3	3.37e-1	7.04e-2	1.56e-1	5.68e-3	1.02e0	8.24e-2	1.47e-1	3.33e-3	1.66e-1	2.46e-2	9.40e-1	2.08e-2	8.00e-1	8.70e-2
	15	8.53e-1	7.94e-2	1.73e-1	6.24e-3	4.02e-1	5.38e-2	1.54e-1	4.77e-3	1.03e0	2.41e-2	1.56e-1	2.00e-3	1.37e-1	5.97e-3	1.37e0	1.11e-2	1.21e0	1.58e-1
<i>f</i> ₉	5	8.37e-2	4.65e-3	1.27e-1	8.24e-3	4.36e-1	1.69e-1	5.74e-1	3.17e-1	9.95e-1	1.53e-2	1.45e0	3.06e-1	8.25e-1	5.36e-1	1.42e-1	5.09e-3	4.61e-1	1.29e-1
	10	5.10e-1	9.74e-3	1.77e-1	8.20e-3	7.10e-1	1.16e-1	7.11e+1	8.76e+1	1.05e0	1.21e-1	1.40e0	4.90e-2	2.46e+1	2.31e+1	1.06e0	1.54e0	8.41e-1	3.00e-1
	15	6.45e-1	1.04e-1	1.51e-1	5.40e-3	3.75e-1	6.34e-2	8.82e-1	2.81e-1	3.17e0	4.71e0	5.86e0	5.65e0	3.71e-1	2.45e-1	3.09e0	4.75e0	1.23e0	2.78e-1
<i>f</i> ₁₀	5	4.48e-1	1.60e-2	4.71e-1	1.09e-2	4.57e-1	1.33e-2	9.34e-1	6.26e-2	5.56e-1	1.73e-2	6.13e-1	4.19e-2	5.21e-1	8.75e-3	1.22e0	3.47e-3	4.67e-1	5.74e-2
	10	1.04e0	4.56e-2	1.20e0	5.94e-2	1.07e0	6.83e-2	1.75e0	8.52e-2	1.09e0	3.43e-2	1.25e0	5.03e-2	1.22e0	8.35e-2	2.62e0	9.16e-2	1.27e0	7.76e-2
	15	1.75e0	3.38e-1	1.96e0	8.53e-2	1.55e0	4.11e-2	2.02e0	2.96e-2	1.49e0	2.25e-2	2.15e0	1.57e-1	1.62e0	1.43e-1	3.13e0	1.47e-1	1.83e0	6.70e-2
<i>f</i> ₁₁	5	6.67e-1	1.53e-2	8.25e-1	1.72e-2	8.25e-1	1.11e-2	8.92e-1	1.17e-1	1.30e0	3.19e-2	1.24e0	1.94e-1	6.75e-1	4.02e-2	5.13e0	2.96e-2	1.70e0	5.31e-1
	10	2.23e0	2.24e0	2.56e0	4.39e-1	4.97e0	1.64e0	2.01e0	2.30e-1	5.81e0	1.71e-1	2.77e0	2.05e-1	2.22e0	4.20e-1	1.67e+1	3.10e-2	6.93e0	2.55e0
	15	7.95e0	3.20e0	4.68e-1	6.22e-1	1.04e+1	2.84e0	8.80e-1	3.24e-1	9.99e0	1.29e0	5.73e0	9.13e-1	5.81e0	1.46e0	2.73e+1	9.79e-2	1.80e+1	3.81e0
<i>f</i> ₁₂	5	1.07e0	5.65e-2	1.12e0	7.95e-3	1.12e0	6.14e-3	1.32e0	4.26e-2	1.16e0	1.25e-2	1.09e0	5.62e-3	1.17e0	1.96e-2	1.56e0	4.08e-2	1.12e0	2.23e-3
	10	4.64e0	1.98e-1	4.69e0	1.44e-2	4.59e0	1.58e-2	4.92e0	7.22e-2	4.11e0	4.39e-2	4.20e0	2.37e-2	4.57e0	3.01e-2	8.89e0	2.90e-1	4.52e0	4.28e-2
	15	7.45e0	6.82e-1	7.62e0	1.66e-1	7.92e0	3.37e-1	8.23e0	1.49e-1	6.70e0	8.06e-2	6.86e0	4.03e-2	6.53e0	9.93e-2	1.50e+1	1.51e0	7.17e0	2.19e-1
<i>f</i> ₁₃	5	1.09e-1	1.07e-2	1.30e-1	6.74e-3	2.59e-1	2.50e-2	1.71e-1	2.12e-2	7.65e-1	2.31e-2	3.51e-1	1.86e-1	2.24e-1	2.55e-2	1.74e-1	6.19e-3	6.85e-1	1.82e-1
	10	2.39e-1	3.28e-2	1.22e-1	7.21e-3	2.18e-1	2.61e-2	1.29e-1	1.62e-2	1.11e0	1.77e-1	3.18e-1	9.29e-2	1.45e-1	1.23e-2	9.97e-1	1.09e-1	8.95e-1	1.88e-1
	15	3.32e-1	1.53e-1	1.50e-1	9.25e-3	3.10e-1	7.77e-2	1.06e-1	2.80e-3	1.47e0	1.92e-1	5.81e-1	5.87e-2	1.12e-1	9.66e-3	1.47e0	1.79e-1	1.11e0	4.23e-1
<i>f</i> ₁₄	5	3.56e-1	6.24e-3	3.85e-1	4.24e-2	1.49e0	1.03e0	1.01e0	1.23e-1	1.65e0	9.10e-1	7.33e-1	2.18e-1	5.46e-1	5.58e-2	7.67e-1	2.44e-1	7.92e-1	1.82e-1
	10	5.98e-1	5.46e-2	6.76e-1	8.35e-2	2.54e0	2.23e0	6.74e0	4.47e0	1.08e0	2.17e-1	2.00e0	1.91e0	9.66e0	2.34e0	5.55e-1	2.65e-1	6.36e-1	4.41e-2
	15	6.36e-1	6.69e-2	6.04e-1	6.46e-2	1.33e0	8.57e-2	3.71e0	4.86e0	1.16e0	7.51e-2	7.57e0	1.31e+1	1.11e+1	2.54e0	9.46e-1	1.44e-1	7.72e-1	1.51e-1
<i>f</i> ₁₅	5	4.72e-1	4.57e-2	6.13e-1	2.57e-2	1.18e0	4.46e-2	1.97e+1	3.82e0	8.57e-1	5.14e-2	1.01e0	7.63e-2	4.15e0	1.94e0	5.80e-1	2.14e-2	5.88e-1	5.21e-2
	10	9.52e-1	3.95e-2	8.52e-1	5.04e-2	1.24e0	2.85e-1	9.37e+1	1.39e+1	7.65e-1	1.85e-1	7.60e-1	5.90e-2	7.02e0	8.52e0	9.77e-1	2.34e-2	9.76e-1	5.86e-2
	15	1.03e0	3.85e-2	1.35e0	7.91e-2	3.37e0	7.25e-1	1.07e+2	1.42e+1	1.31e0	7.08e-3	1.30e0	3.77e-3	1.03e+2	5.96e+1	1.07e0	2.36e-2	1.18e0	3.13e-2
Rank	5	1.20		3.37		5.17		5.87		6.53		4.67		5.13		6.80		6.27	
	10	3.40		3.73		5.07		5.80</											

TABLE III
STATISTICS FOR NHV: MEAN, STD, FRIEDMAN MEAN RANKS AND *t*-TESTS OF 9 ALGORITHMS AVERAGED USING 20 INDEPENDENT RUNS

	CLIA		AR-MOEA		NSGA-III		NSGA-II		IBEA		GrEA		KnEA		MOEA/D		RVEA		
	Mean	Std	Mean	Std	Mean	Std	Mean	Std	Mean	Std	Mean	Std	Mean	Std	Mean	Std	Mean	Std	
f_1	5	1.26e-2	8.83e-5	8.82e-3	2.27e-4	5.31e-3	4.93e-4	6.32e-3	1.82e-4	9.78e-3	1.34e-4	9.94e-3	1.13e-4	1.06e-2	9.42e-5	5.58e-3	4.39e-4	2.29e-3	6.22e-4
	10	4.41e-7	5.84e-9	7.00e-7	9.23e-7	4.89e-7	4.24e-8	0.00e0	0.00e0	4.41e-7	3.02e-8	6.22e-7	4.82e-7	4.11e-7	1.28e-7	3.51e-8	1.76e-10	4.95e-9	3.41e-9
	15	1.12e-11	3.38e-13	0.00e0	0.00e0	6.04e-12	7.08e-13	0.00e0	0.00e0	7.04e-12	5.21e-13	0.00e0	0.00e0	0.00e0	0.00e0	9.16e-14	2.81e-15	3.23e-14	2.04e-14
f_2	5	1.96e-1	9.04e-4	1.67e-1	2.72e-3	1.55e-1	4.78e-3	1.52e-1	2.50e-3	1.87e-1	4.98e-4	1.95e-1	1.20e-3	1.89e-1	1.56e-3	4.41e-1	1.14e-1	7.23e-4	1.52e-1
	10	1.97e-1	1.67e-2	2.17e-1	1.91e-3	2.16e-1	1.11e-2	1.87e-1	6.78e-3	2.17e-1	4.67e-3	2.43e-1	1.03e-3	1.69e-1	3.56e-3	2.09e-1	3.30e-4	1.86e-1	4.67e-3
	15	2.13e-1	1.41e-3	1.48e-1	8.51e-3	1.43e-1	1.71e-2	1.08e-1	1.01e-2	2.17e-1	9.26e-4	2.15e-1	1.78e-3	1.10e-1	1.89e-2	1.81e-1	9.92e-4	5.30e-2	2.11e-2
f_3	5	1.00e0	1.65e-3	9.99e-1	1.79e-4	9.94e-1	9.87e-3	8.99e-1	6.24e-3	5.58e-1	4.09e-1	3.77e-1	3.07e-1	9.68e-1	2.99e-2	9.84e-1	1.93e-3	9.96e-1	1.49e-3
	10	1.00e0	1.29e-3	6.77e-1	4.57e-1	0.00e0	0.00e0	0.00e0	0.00e0	8.81e-1	5.36e-2	0.00e0	0.00e0	0.00e0	0.00e0	9.67e-1	1.53e-3	9.99e-1	1.02e-3
	15	1.00e0	3.13e-4	4.94e-1	4.87e-1	9.53e-1	1.03e-1	0.00e0	0.00e0	9.55e-1	5.27e-2	0.00e0	0.00e0	0.00e0	0.00e0	9.67e-1	1.71e-4	9.97e-1	4.37e-3
f_4	5	9.03e-2	3.77e-3	7.13e-2	5.42e-3	6.39e-2	8.46e-3	7.86e-2	3.53e-3	6.76e-3	1.41e-3	1.19e-1	1.47e-3	1.08e-1	4.80e-3	1.66e-2	5.49e-3	9.35e-3	6.57e-3
	10	8.54e-7	1.22e-7	2.80e-6	8.52e-7	2.05e-4	1.73e-5	3.04e-5	1.21e-5	2.51e-8	5.61e-8	4.56e-4	2.73e-5	1.16e-4	2.59e-5	3.17e-8	9.70e-9	6.23e-8	2.49e-8
	15	4.84e-12	3.53e-13	3.84e-11	3.67e-11	1.88e-7	6.04e-9	0.00e0	0.00e0	6.07e-14	1.36e-13	5.63e-7	2.96e-7	6.83e-9	1.26e-8	9.87e-14	9.08e-15	2.18e-13	1.19e-13
f_5	5	1.96e-1	3.55e-2	7.75e-1	1.96e-2	7.80e-1	3.19e-4	3.19e-4	1.23e-2	7.76e-1	3.43e-2	7.71e-1	4.28e-2	7.75e-1	2.56e-3	4.41e-1	1.14e-1	7.61e-1	4.10e-2
	10	9.62e-1	1.56e-2	9.64e-1	2.12e-3	9.68e-1	1.75e-4	0.00e0	0.00e0	9.73e-1	3.55e-4	9.70e-1	2.45e-4	9.54e-1	6.58e-3	4.33e-1	1.41e-2	9.54e-1	1.96e-3
	15	9.77e-1	4.33e-2	9.26e-1	3.42e-2	9.90e-1	1.97e-3	0.00e0	0.00e0	9.96e-1	1.51e-4	9.93e-1	1.05e-4	9.94e-1	9.25e-5	3.10e-1	5.50e-2	9.44e-1	1.10e-2
f_6	5	1.29e-1	3.20e-4	1.29e-1	2.17e-4	1.26e-1	4.30e-4	1.29e-1	1.38e-4	1.14e-1	6.83e-3	1.18e-1	2.97e-4	1.28e-1	5.83e-4	1.23e-1	2.38e-3	1.14e-1	1.09e-3
	10	9.80e-2	4.96e-4	9.08e-2	1.34e-2	8.24e-2	7.84e-3	2.84e-2	3.89e-2	9.28e-2	1.81e-3	1.99e-2	3.02e-2	0.00e0	0.00e0	8.54e-2	3.25e-2	8.97e-2	5.66e-3
	15	9.28e-2	1.12e-3	7.12e-2	2.32e-2	6.50e-2	1.96e-2	8.27e-3	1.85e-2	4.46e-2	4.09e-2	2.50e-3	5.58e-3	0.00e0	0.00e0	4.00e-2	4.99e-2	9.20e-2	9.11e-4
f_7	5	2.58e-1	5.37e-3	2.37e-1	1.96e-3	2.37e-1	3.48e-3	1.91e-1	4.73e-3	2.63e-1	8.51e-3	2.59e-1	2.34e-3	2.56e-1	3.46e-3	8.19e-3	2.76e-3	2.15e-1	2.99e-4
	10	1.82e-1	1.75e-2	1.56e-1	1.00e-2	1.77e-1	4.91e-3	2.82e-6	5.04e-6	1.97e-1	5.82e-3	2.18e-1	2.26e-3	8.57e-2	2.77e-2	3.17e-4	3.88e-4	1.50e-1	1.42e-2
	15	4.78e-2	3.27e-2	5.01e-2	3.05e-2	1.06e-1	4.05e-2	9.55e-10	2.13e-9	1.62e-1	1.19e-2	1.88e-1	8.40e-4	5.37e-6	1.20e-5	6.19e-8	8.95e-8	1.10e-1	5.55e-2
f_8	5	1.25e-1	5.99e-4	1.16e-1	9.92e-4	9.22e-2	4.90e-3	1.06e-1	2.35e-3	5.67e-3	6.72e-4	1.11e-1	2.46e-3	1.02e-1	1.60e-2	1.04e-1	9.08e-4	7.65e-2	4.23e-3
	10	5.40e-3	2.20e-3	1.06e-2	9.07e-5	8.81e-3	5.26e-4	8.89e-3	2.10e-4	6.92e-5	1.30e-5	9.78e-3	9.92e-5	1.01e-2	2.62e-4	6.52e-3	9.68e-5	4.97e-3	6.55e-4
	15	2.77e-4	4.86e-5	6.16e-4	1.84e-5	5.08e-4	2.19e-5	5.18e-4	1.91e-5	2.62e-7	5.87e-7	5.61e-4	1.68e-5	6.24e-4	2.95e-5	3.17e-4	5.15e-6	1.57e-4	4.12e-5
f_9	5	3.21e-1	3.08e-3	2.97e-1	4.02e-3	1.92e-1	4.63e-2	1.63e-1	5.41e-2	4.78e-2	2.96e-3	3.83e-2	2.68e-2	1.29e-1	7.49e-2	2.85e-1	3.35e-3	1.69e-1	3.12e-2
	10	5.96e-3	2.28e-4	1.57e-2	2.95e-4	7.21e-3	1.81e-3	2.33e-5	5.21e-5	8.14e-4	1.21e-4	2.62e-3	3.53e-4	3.88e-4	8.67e-4	1.12e-2	6.28e-3	4.25e-3	1.59e-3
	15	4.77e-4	6.06e-5	1.26e-3	3.17e-5	8.21e-4	1.40e-4	3.13e-4	8.68e-5	2.40e-5	1.46e-5	7.18e-5	6.74e-5	8.93e-4	3.92e-4	6.14e-4	3.43e-4	2.52e-4	7.47e-5
f_{10}	5	9.76e-1	3.43e-2	9.98e-1	7.67e-5	9.98e-1	7.50e-5	9.65e-1	7.22e-3	9.86e-1	3.31e-3	9.71e-1	8.63e-3	9.88e-1	8.96e-4	9.40e-1	1.35e-2	9.96e-1	1.99e-3
	10	9.98e-1	4.33e-4	9.99e-1	6.14e-4	9.83e-1	3.51e-2	9.96e-1	1.63e-3	9.93e-1	9.08e-4	9.85e-1	4.62e-3	9.98e-1	6.40e-4	5.39e-1	1.10e-1	9.97e-1	5.29e-4
	15	9.97e-1	1.37e-3	9.99e-1	4.21e-4	1.00e0	8.94e-5	1.00e0	1.97e-4	9.96e-1	1.09e-3	9.93e-1	1.38e-3	9.98e-1	5.95e-4	5.87e-1	1.82e-1	9.99e-1	4.89e-4
f_{11}	5	9.95e-1	5.83e-4	9.96e-1	4.21e-4	9.96e-1	7.86e-4	9.81e-1	5.32e-3	9.75e-1	6.24e-3	9.71e-1	2.77e-3	9.91e-1	9.90e-4	9.53e-1	3.29e-3	9.89e-1	1.39e-3
	10	9.96e-1	1.96e-3	9.96e-1	1.27e-3	9.97e-1	7.56e-4	9.97e-1	1.29e-3	9.86e-1	2.81e-3	9.80e-1	3.93e-3	9.94e-1	6.66e-4	9.37e-1	2.82e-3	9.88e-1	3.21e-3
	15	9.99e-1	7.88e-2	9.96e-1	1.35e-3	9.94e-1	4.12e-3	9.98e-1	5.42e-4	9.91e-1	2.01e-3	9.73e-1	4.09e-3	9.94e-1	3.53e-4	9.42e-1	8.84e-4	9.72e-1	5.67e-3
f_{12}	5	7.17e-1	2.53e-2	7.13e-1	2.99e-2	7.15e-1	1.35e-2	5.53e-1	4.23e-2	7.34e-1	1.13e-2	7.48e-1	3.08e-3	7.49e-1	4.98e-3	6.05e-1	1.93e-2	7.40e-1	4.57e-3
	10	8.07e-1	3.17e-2	8.55e-1	2.08e-2	8.95e-1	5.46e-3	6.22e-1	3.83e-2	8.88e-1	3.49e-3	9.00e-1	2.00e-3	9.13e-1	2.41e-3	3.35e-1	1.27e-1	8.89e-1	9.90e-3
	15	6.56e-1	6.24e-2	8.72e-1	2.79e-2	8.53e-1	9.44e-2	6.35e-1	2.69e-2	9.12e-1	8.22e-3	9.19e-1	3.36e-3	9.35e-1	8.89e-3	2.69e-1	7.77e-2	8.36e-1	3.39e-2
f_{13}	5	2.73e-1	7.20e-3	2.53e-1	4.10e-3	2.00e-1	7.12e-3	2.24e-1	1.09e-2	2.54e-3	6.69e-4	1.53e-1	8.40e-2	2.06e-1	2.16e-2	2.31e-1	1.21e-2	1.53e-1	1.54e-2
	10	8.93e-2	1.03e-2	1.35e-1	2.93e-3	1.16e-1	5.34e-3	1.21e-1	5.32e-3	2.30e-5	4.91e-5	6.99e-2	4.68e-2	1.12e-1	7.31e-3	5.49e-2	3.62e-2	7.91e-2	2.21e-2
	15	5.51e-2	7.68e-3	9.22e-2	1.47e-3	4.03e-2	2.98e-2	8.51e-2	1.47e-3	6.33e-9	1.42e-8	3.93e-4	3.35e-4	8.39e-2	2.30e-3	3.48e-2	2.48e-2	5.64e-2	8.96e-3
f_{14}	5	5.52e-1	7.20e-3	5.30e-1	3.18e-2	1.17e-1	1.55e-1	1.63e-2	1.82e-2	6.75e-3	1.51e-2	3.05e-1	2.56e-1	4.23e-1	9.84e-2	1.87e-1	2.13e-1	2.05e-1	1.97e-1
	10	5.44e-1	1.03e-2	5.07e-1	1.45e-1	4.50e-2	1.01e-1	0.00e0	0.00e0	8.73e-2	1.23e-1	8.09e-2	1.03e-1	0.00e0	0.00e0	7.54e-1	3.73e-1	6.65e-1	7.15e-2
	15	5.38e-1	7.68e-3	6.14e-1	9.45e-2	0.00e0	0.00e0	1.62e-2	3.62e-2	2.00e-2	3.20e-2	5.72e-2	1.28e-1	0.00e0	0.00e0	1.71e-1	1.20e-1	3.90e-1	1.97e-1
f_{15}	5	2.87e-2	9.35e-3	1.96e-2	3.69e-3	7.07e-6	1.58e-5	0.00e0	0.00e0	1.25e-3	7.21e-4	1.04e-3	1.43e-3	2.84e-8	6.35e-8	3.86e-2	4.90e-3	2.34e-2	4.54e-3
	10	6.00e-6	1.07e-8	3.93e-6	3.00e-6	0.00e0	0.00e0	0.00e0	0.00e0	2.92e-5	2.92e-5	3.00e-5	3.41e-5	0.00e0	0.00e0	2.92e-6	1.29e-6	1.81e-6	1.21e-6
	15	1.49e-11	1.08e-11	3.15e-17	1.41e-16	0.00e0	0.00e0	0.00e0	0.00e0	6.13e-16	6.07e-16	1.07e-15	3.92e-16	0.00e0	0.00e0	2.19e-10	2.08e-10	1.85e-13	1.07e-13
Rank	5	7.87		6.60		4.83		3.50		3.77		4.90		5.67		3.80		3.97	
	10																		

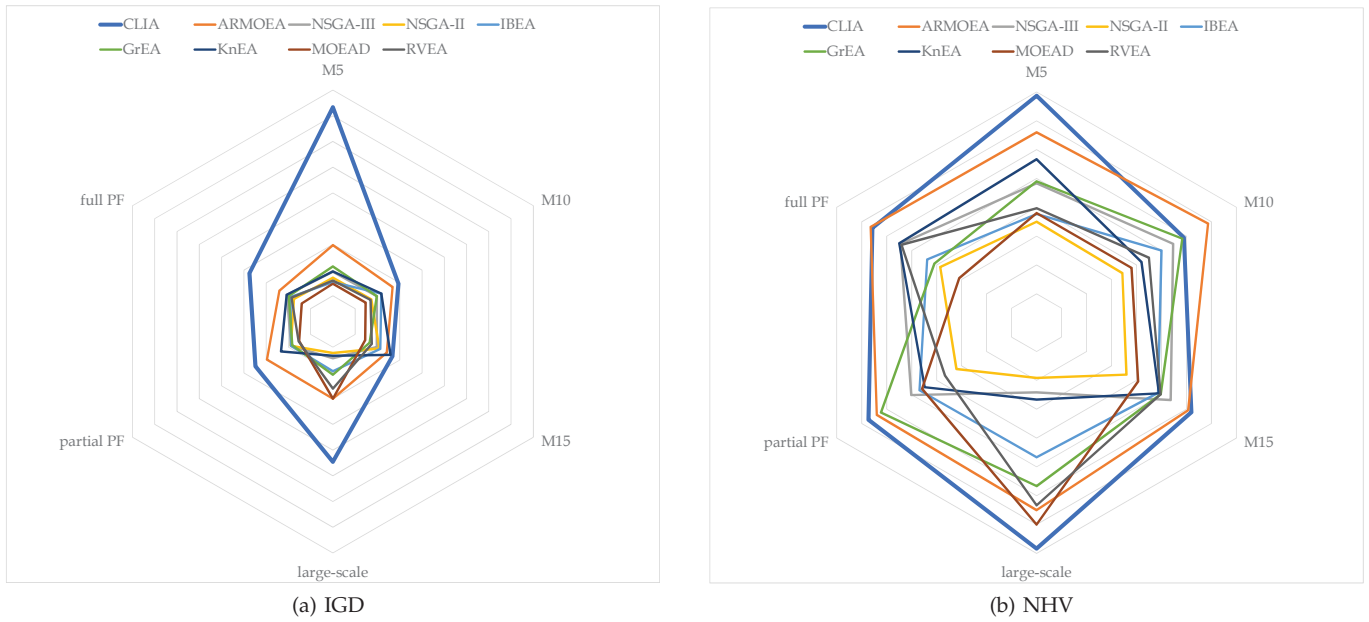


Fig. 7. The radar diagrams for the specified performance on each category of benchmark functions using the metrics of IGD and NHV respectively

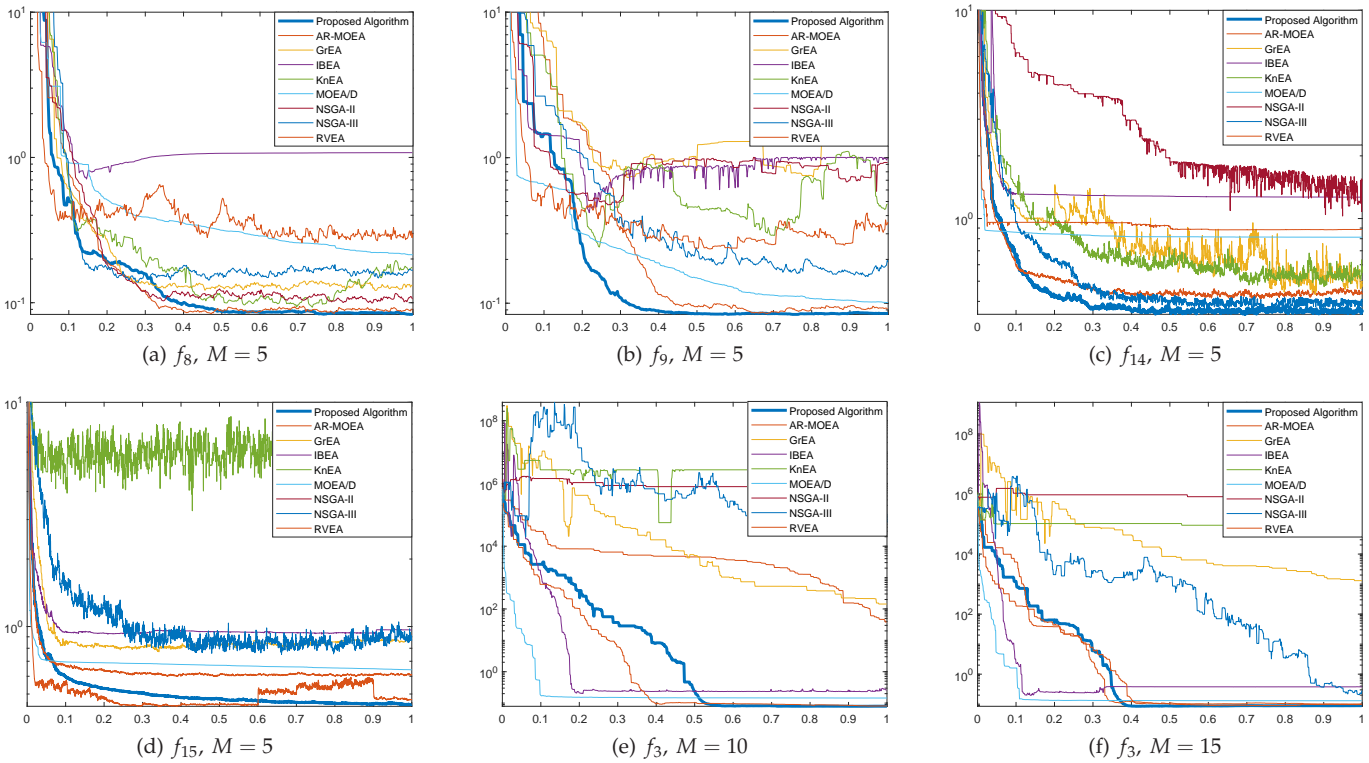


Fig. 8. IGD curves of all compared algorithms for six test cases

point incremental learning. In CLIA, a cascade clustering mechanism functions as the selection operator, ensuring the proximity and diversity of the population using the reference lines provided by the learning process. To provide the clustering process with properly distributed reference lines, CLIA is also integrated with the reference point incremental learning process, where the proper

generation of reference points are gradually estimated using the feedbacks from the clustering process. In characteristic studies, analyses have shown that the covering of the true PF by the population is relatively satisfactory. Comparative experimental results with the state-of-the-art algorithms also show that CLIA obtains competitive results on the CEC'2018 many-objective benchmark func-

tions. Moreover, we have compared, analyzed and discussed that the proposed algorithm CLIA has relatively high efficiency and stable convergence patterns. It can be concluded that the proposed algorithm CLIA is effective, efficient and stable in dealing with the MaOPs and in addressing some of the existing problems in MOEAs.

ACKNOWLEDGMENT

The authors are thankful to the creators of the MATLAB platform PlatEMO for bringing the convenience to researchers' experiments.

The authors are grateful to the support of the National Natural Science Foundation of China (61572104, 61103146, 61425002, 61751203), the Fundamental Research Funds for the Central Universities (DUT17JC04), and the Project of the Key Laboratory of Symbolic Computation and Knowledge Engineering of Ministry of Education, Jilin University (93K172017K03).

REFERENCES

- [1] H. Louafi, S. Coulombe, and M. Cheriet, "Multi-objective optimization in dynamic content adaptation of slide documents," *IEEE Transactions on Services Computing*, vol. 10, no. 2, pp. 231–243, 2017.
- [2] L. Li, L. Jiao, J. Zhao, R. Shang, and M. Gong, "Quantum-behaved discrete multi-objective particle swarm optimization for complex network clustering," *Pattern Recognition*, vol. 63, pp. 1–14, 2017.
- [3] A. C. Ferreira, M. L. Nunes, J. C. Teixeira, L. A. Martins, S. F. Teixeira, and S. A. Nebra, "Design of a solar dish stirling cogeneration system: Application of a multi-objective optimization approach," *Applied Thermal Engineering*, vol. 123, pp. 646–657, 2017.
- [4] A. Zhou, B.-Y. Qu, H. Li, S.-Z. Zhao, P. N. Suganthan, and Q. Zhang, "Multiobjective evolutionary algorithms: A survey of the state of the art," *Swarm and Evolutionary Computation*, vol. 1, no. 1, pp. 32–49, 2011.
- [5] M. Li, S. Yang, and X. Liu, "Bi-goal evolution for many-objective optimization problems," *Artificial Intelligence*, vol. 228, no. Supplement C, pp. 45–65, 2015.
- [6] K. Deb, A. Pratap, S. Agarwal, and T. Meyarivan, "A fast and elitist multiobjective genetic algorithm: NSGA-II," *IEEE Transactions on Evolutionary Computation*, vol. 6, no. 2, pp. 182–197, 2002.
- [7] M. Kim, T. Hiroyasu, M. Miki, and S. Watanabe, *SPEA2+: Improving the Performance of the Strength Pareto Evolutionary Algorithm 2*. Berlin, Heidelberg: Springer Berlin Heidelberg, 2004, pp. 742–751.
- [8] D. W. Corne, N. R. Jerram, J. D. Knowles, and M. J. Oates, "PESA-II: Region-based selection in evolutionary multiobjective optimization," in *Proceedings of the 3rd Annual Conference on Genetic and Evolutionary Computation*, 2001, pp. 283–290.
- [9] R. C. Purshouse and P. J. Fleming, "On the evolutionary optimization of many conflicting objectives," *IEEE Transactions on Evolutionary Computation*, vol. 11, no. 6, pp. 770–784, 2007.
- [10] H. Wang, Y. Jin, and X. Yao, "Diversity assessment in many-objective optimization," *IEEE Transactions on Cybernetics*, vol. 47, no. 6, pp. 1510–1522, 2017.
- [11] K. Bringmann, T. Friedrich, C. Igel, and T. VoB, "Speeding up many-objective optimization by monte carlo approximations," *Artificial Intelligence*, vol. 204, pp. 22–29, 2013.
- [12] X. Zhang, Y. Tian, and Y. Jin, "A knee point-driven evolutionary algorithm for many-objective optimization," *IEEE Transactions on Evolutionary Computation*, vol. 19, no. 6, pp. 761–776, 2015.
- [13] W. Hu, G. G. Yen, and G. Luo, "Many-objective particle swarm optimization using two-stage strategy and parallel cell coordinate system," *IEEE Transactions on Cybernetics*, vol. 47, no. 6, pp. 1446–1459, 2017.
- [14] D. Brockhoff, T. Friedrich, N. Hebbinghaus, C. Klein, F. Neumann, and E. Zitzler, "On the effects of adding objectives to plateau functions," *IEEE Transactions on Evolutionary Computation*, vol. 13, no. 3, pp. 591–603, 2009.
- [15] Y. N. Kou, J. H. Zheng, Z. Li, and Q. H. Wu, "Many-objective optimization for coordinated operation of integrated electricity and gas network," *Journal of Modern Power Systems and Clean Energy*, vol. 5, no. 3, pp. 350–363, 2017.
- [16] B. D. Raja, R. Jhala, and V. Patel, "Many-objective optimization of cross-flow plate-fin heat exchanger," *International Journal of Thermal Sciences*, vol. 118, pp. 320–339, 2017.
- [17] R. Cheng, T. Rodemann, M. Fischer, M. Olhofer, and Y. Jin, "Evolutionary many-objective optimization of hybrid electric vehicle control: From general optimization to preference articulation," *IEEE Transactions on Emerging Topics in Computational Intelligence*, vol. 1, no. 2, pp. 97–111, 2017.
- [18] D. Hadka and P. Reed, "Diagnostic assessment of search controls and failure modes in many-objective evolutionary optimization," *Evolutionary Computation*, vol. 20, no. 3, pp. 423–452, 2012.
- [19] —, "Borg: An auto-adaptive many-objective evolutionary computing framework," *Evolutionary Computation*, vol. 21, no. 2, pp. 231–259, 2013.
- [20] O. Teytaud, "On the hardness of offline multi-objective optimization," *Evolutionary Computation*, vol. 15, no. 4, pp. 475–491, 2007.
- [21] X. Zou, Y. Chen, M. Liu, and L. Kang, "A new evolutionary algorithm for solving many-objective optimization problems," *IEEE Transactions on Systems, Man, and Cybernetics, Part B (Cybernetics)*, vol. 38, no. 5, pp. 1402–1412, 2008.
- [22] K. Deb, M. Mohan, and S. Mishra, "Evaluating the ϵ -domination based multi-objective evolutionary algorithm for a quick computation of pareto-optimal solutions," *Evolutionary Computation*, vol. 13, no. 4, pp. 501–525, 2005.
- [23] C. Dai, Y. Wang, and L. Hu, "An improved α -dominance strategy for many-objective optimization problems," *Soft Computation*, vol. 20, no. 3, pp. 1105–1111, 2016.
- [24] Y. Yuan, H. Xu, and B. Wang, "An improved NSGA-III procedure for evolutionary many-objective optimization," in *Proceedings of the 2014 Annual Conference on Genetic and Evolutionary Computation*, 2014, pp. 661–668.
- [25] N. Kowatari, A. Oyama, H. E. Aguirre, and K. Tanaka, *A Study on Large Population MOEA Using Adaptive ϵ -Box Dominance and Neighborhood Recombination for Many-Objective Optimization*. Berlin, Heidelberg: Springer Berlin Heidelberg, 2012, pp. 86–100.
- [26] H. Sato, H. E. Aguirre, and K. Tanaka, *Controlling Dominance Area of Solutions and Its Impact on the Performance of MOEAs*. Berlin, Heidelberg: Springer Berlin Heidelberg, 2007, pp. 5–20.
- [27] M. Farina and P. Amato, "A fuzzy definition of "optimality" for many-criteria optimization problems," *IEEE Transactions on Systems, Man, and Cybernetics - Part A: Systems and Humans*, vol. 34, no. 3, pp. 315–326, 2004.
- [28] M. Li, S. Yang, X. Liu, and R. Shen, *A Comparative Study on Evolutionary Algorithms for Many-Objective Optimization*. Berlin, Heidelberg: Springer Berlin Heidelberg, 2013, pp. 261–275.
- [29] M. Li, J. Zheng, K. Li, Q. Yuan, and R. Shen, *Enhancing Diversity for Average Ranking Method in Evolutionary Many-Objective Optimization*. Berlin, Heidelberg: Springer Berlin Heidelberg, 2010, pp. 647–656.
- [30] Z. He and G. G. Yen, "A new fitness evaluation method based on fuzzy logic in multiobjective evolutionary algorithms," in *2012 IEEE Congress on Evolutionary Computation*, June 2012, pp. 1–8.
- [31] Z. He, G. G. Yen, and J. Zhang, "Fuzzy-based pareto optimality for many-objective evolutionary algorithms," *IEEE Transactions on Evolutionary Computation*, vol. 18, no. 2, pp. 269–285, 2014.
- [32] R. Wang, R. C. Purshouse, and P. J. Fleming, "On finding well-spread pareto optimal solutions by preference-inspired co-evolutionary algorithm," in *Proceedings of the 15th Annual Conference on Genetic and Evolutionary Computation*, 2013, pp. 695–702.
- [33] —, "Preference-inspired coevolutionary algorithms for many-objective optimization," *IEEE Transactions on Evolutionary Computation*, vol. 17, no. 4, pp. 474–494, 2013.
- [34] F. di Pierro, S. T. Khu, and D. A. Savic, "An investigation on preference order ranking scheme for multiobjective evolutionary optimization," *IEEE Transactions on Evolutionary Computation*, vol. 11, no. 1, pp. 17–45, 2007.
- [35] S. Yang, M. Li, X. Liu, and J. Zheng, "A grid-based evolutionary algorithm for many-objective optimization," *IEEE Transactions on Evolutionary Computation*, vol. 17, no. 5, pp. 721–736, 2013.
- [36] U. K. Wickramasinghe and X. Li, "Using a distance metric to guide PSO algorithms for many-objective optimization," in *Proceedings of the 11th Annual Conference on Genetic and Evolutionary Computation*, 2009, pp. 667–674.

- [37] M. Garza-Fabre, G. Toscano-Pulido, and C. A. C. Coello, "Two novel approaches for many-objective optimization," in *IEEE Congress on Evolutionary Computation*, July 2010, pp. 1–8.
- [38] S. Kukkonen and J. Lampinen, "Ranking-dominance and many-objective optimization," in *2007 IEEE Congress on Evolutionary Computation*, Sept 2007, pp. 3983–3990.
- [39] S. F. Adra and P. J. Fleming, "Diversity management in evolutionary many-objective optimization," *IEEE Transactions on Evolutionary Computation*, vol. 15, no. 2, pp. 183–195, 2011.
- [40] M. Li, S. Yang, and X. Liu, "Diversity comparison of pareto front approximations in many-objective optimization," *IEEE Transactions on Cybernetics*, vol. 44, no. 12, pp. 2568–2584, 2014.
- [41] L. Cai, S. Qu, Y. Yuan, and X. Yao, "A clustering-ranking method for many-objective optimization," *Applied Soft Computing*, vol. 35, pp. 681 – 694, 2015.
- [42] H. K. Singh, A. Isaacs, and T. Ray, "A pareto corner search evolutionary algorithm and dimensionality reduction in many-objective optimization problems," *IEEE Transactions on Evolutionary Computation*, vol. 15, no. 4, pp. 539–556, 2011.
- [43] E. Zitzler and S. Künzli, *Indicator-Based Selection in Multiobjective Search*. Springer Berlin Heidelberg, 2004, pp. 832–842.
- [44] N. Beume, B. Naujoks, and M. Emmerich, "SMS-EMOA: Multi-objective selection based on dominated hypervolume," *European Journal of Operational Research*, vol. 181, no. 3, pp. 1653 – 1669, 2007.
- [45] S. Rostami and F. Neri, "A fast hypervolume driven selection mechanism for many-objective optimization problems," *Swarm and Evolutionary Computation*, vol. 34, pp. 50 – 67, 2017.
- [46] K. Bringmann and T. Friedrich, "An efficient algorithm for computing hypervolume contributions," *Evolutionary Computation*, vol. 18, no. 3, pp. 383–402, 2010.
- [47] S. Jiang, J. Zhang, Y. S. Ong, A. N. Zhang, and P. S. Tan, "A simple and fast hypervolume indicator-based multiobjective evolutionary algorithm," *IEEE Transactions on Cybernetics*, vol. 45, no. 10, pp. 2202–2213, 2015.
- [48] O. Schütze, X. Esquivel, A. Lara, and C. A. C. Coello, "Using the averaged hausdorff distance as a performance measure in evolutionary multiobjective optimization," *IEEE Transactions on Evolutionary Computation*, vol. 16, no. 4, pp. 504–522, 2012.
- [49] R. Hernández Gómez and C. A. Coello Coello, "Improved metaheuristic based on the R2 indicator for many-objective optimization," in *Proceedings of the 2015 Annual Conference on Genetic and Evolutionary Computation*, 2015, pp. 679–686.
- [50] H. Trautmann, T. Wagner, and D. Brockhoff, *R2-EMOA: Focused Multiobjective Search Using R2-Indicator-Based Selection*. Berlin, Heidelberg: Springer Berlin Heidelberg, 2013, pp. 70–74.
- [51] Y. Tian, R. Cheng, X. Zhang, F. Cheng, and Y. Jin, "An indicator based multi-objective evolutionary algorithm with reference point adaptation for better versatility," *IEEE Transactions on Evolutionary Computation*, vol. PP, no. 99, pp. 1–1, 2017.
- [52] K. Bringmann and T. Friedrich, "Approximating the volume of unions and intersections of high-dimensional geometric objects," *Computational Geometry*, vol. 43, no. 6, pp. 601 – 610, 2010.
- [53] Y. Sun, G. G. Yen, and Z. Yi, "IGD indicator-based evolutionary algorithm for many-objective optimization problems," *IEEE Transactions on Evolutionary Computation*, vol. PP, no. 99, pp. 1–1, 2018.
- [54] J. Bader and E. Zitzler, "HypE: An algorithm for fast hypervolume-based many-objective optimization," *Evolutionary Computation*, vol. 19, no. 1, pp. 45–76, 2011.
- [55] K. Deb and H. Jain, "An evolutionary many-objective optimization algorithm using reference-point-based nondominated sorting approach, part I: Solving problems with box constraints," *IEEE Transactions on Evolutionary Computation*, vol. 18, no. 4, pp. 577–601, 2014.
- [56] Q. Zhang and H. Li, "MOEA/D: A multiobjective evolutionary algorithm based on decomposition," *IEEE Transactions on Evolutionary Computation*, vol. 11, no. 6, pp. 712–731, 2007.
- [57] S. Jiang, S. Yang, Y. Wang, and X. Liu, "Scalarizing functions in decomposition-based multiobjective evolutionary algorithms," *IEEE Transactions on Evolutionary Computation*, vol. PP, no. 99, pp. 1–1, 2017.
- [58] R. Cheng, Y. Jin, M. Olhofer, and B. Sendhoff, "A reference vector guided evolutionary algorithm for many-objective optimization," *IEEE Transactions on Evolutionary Computation*, vol. 20, no. 5, pp. 773–791, 2016.
- [59] Y. Qi, X. Ma, F. Liu, L. Jiao, J. Sun, and J. Wu, "MOEA/D with adaptive weight adjustment," *Evolutionary Computation*, vol. 22, no. 2, pp. 231–264, 2014.
- [60] H. Jain and K. Deb, "An evolutionary many-objective optimization algorithm using reference-point based nondominated sorting approach, part II: Handling constraints and extending to an adaptive approach," *IEEE Transactions on Evolutionary Computation*, vol. 18, no. 4, pp. 602–622, 2014.
- [61] F.-A. Fortin, S. Grenier, and M. Parizeau, "Generalizing the improved run-time complexity algorithm for non-dominated sorting," in *Proceedings of the 15th Annual Conference on Genetic and Evolutionary Computation*, 2013, pp. 615–622.
- [62] J. C. Platt, "Probabilistic outputs for support vector machines and comparisons to regularized likelihood methods," in *Advances in Large Margin Classifiers*. MIT Press, 1999, pp. 61–74.
- [63] R. Cheng, M. Li, Y. Tian, X. Xiang, X. Zhang, S. Yang, Y. Jin, and X. Yao, "Benchmark functions for CEC'2018 competition on many-objective optimization," CERCIA, School of Computer Science, University of Birmingham Edgbaston, Birmingham B15 2TT, U.K., School of Computer Science and Technology, Anhui University Hefei 230039, China, School of Computer Science and Informatics, De Montfort University Leicester, LE1 9BH, U.K., Department of Computer Science, University of Surrey Guildford, Surrey, GU2 7XH, U.K., Tech. Rep., 2017.
- [64] E. Cheney and D. Kincaid, *The Gram-Schmidt Process*. Jones and Bartlett Learning, 2008, pp. 544–550.
- [65] Y. Tian, R. Cheng, X. Zhang, and Y. Jin, "PlatEMO: A MATLAB platform for evolutionary multi-objective optimization [educational forum]," *IEEE Computational Intelligence Magazine*, vol. 12, no. 4, pp. 73–87, 2017.
- [66] C. P. Diehl and G. Cauwenberghs, "SVM incremental learning, adaptation and optimization," in *Proceedings of the International Joint Conference on Neural Networks*, vol. 4, July 2003, pp. 2685–2690.
- [67] P. Czyżżak and A. Jaskiewicz, "Pareto simulated annealing: A metaheuristic technique for multiple-objective combinatorial optimization," *Journal of Multi-Criteria Decision Analysis*, vol. 7, no. 1, pp. 34–47, 1998.
- [68] C. A. Coello Coello and M. Reyes Sierra, *A Study of the Parallelization of a Coevolutionary Multi-objective Evolutionary Algorithm*. Springer Berlin Heidelberg, 2004, pp. 688–697.
- [69] M. Reyes-Sierra and C. Coello, "A new multi-objective particle swarm optimizer with improved selection and diversity mechanisms," Technical Report EVOCINV-05-2004, Sección de Computación, Depto. de Ingeniería Eléctrica, CINVESTAV-IPN, México, Tech. Rep., 2004.
- [70] E. Zitzler and L. Thiele, "Multiobjective evolutionary algorithms: A comparative case study and the strength pareto approach," *IEEE Transactions on Evolutionary Computation*, vol. 3, no. 4, pp. 257–271, 1999.